

## **APPLICATIONS FOR REMOTE SENSING BY UNMANNED AERIAL VEHICLES IN RECLAMATION MONITORING.**

Jeff Anderson, RPBio  
Melissa Iverson, PAg  
Ben Pearce

Integral Ecology Group Ltd.

### **Abstract**

Mapping by unmanned aerial vehicles (UAVs) is a relatively new tool which is becoming more accessible, with an increasing set of sensors with potential applications in mine reclamation.

UAV mounted multispectral and hyperspectral sensors provide imagery capturing narrow bands within the visible spectra, but also capture imagery in the invisible near-infrared, red-edge spectra, as well as the ultraviolet for hyperspectral. Imagery captured from these cameras are ideal for monitoring of vegetation communities, including through the analysis of vegetation indices, such as the most widely used normalized difference vegetation index (NDVI).

Every year there are better and more cost-effective options for UAV mounted LiDAR sensors, which are able to provide detailed elevation maps of small areas. The best-known uses for UAV mounted LiDAR at mine sites are conducting high-quality cover-depth surveys and as-built site diagrams. These systems can also be used to create highly accurate descriptions of vegetation systems, providing data such as: canopy and sub-canopy heights, tree counts, and aboveground biomass.

Even a small UAV equipped with a simple camera can be a useful tool in reclamation monitoring. Using a Mavic Pro purchased in 2018 for about fifteen hundred dollars, IEG created RGB (visual spectrum) imagery of a reclamation trial area. The RGB imagery was used for semi-autonomous classification of areas which had received a high, medium, or low application of an organic peat amendment as a component of reclamation-cover placement. This classification was then used to assess differences in survival of planted seedlings by peat content, which would have been more difficult using ground-based sampling methods. These methods will allow for assessment of impacts of this uneven distribution of an organic amendment on the success of revegetation efforts over time.

This paper outlines reclamation monitoring applications of UAV technology, including a case study from our own work.

### **Key Words**

Remote sensing, UAV, LiDAR, Multispectral, Automatic image classification, Reclamation monitoring.

### **Introduction**

Technology is rapidly progressing in the fields of unmanned aerial vehicles (UAVs) and in the sensors they can carry. Along with the advances in technology, these tools have become more user-friendly, particularly as it pertains to the UAV flight and data collection. It is now normal that data collection

occurs with the UAV autonomously following a pre-determined flight plan developed in relatively easy-to-use software (Valavanis Kimon P. and Vachtsevanos, 2015). Data processing ranges from quite easy for simple or cloud-based analysis, to extremely difficult for advanced applications. With these advances, UAV-based remote-sensing is becoming more accessible for use and has more possible applications in the field of mine reclamation (Park and Choi, 2020).

Though there are additional sensors which may be useful for narrower applications, this paper will cover the following sensor technologies; LiDAR, photogrammetry, and multispectral or hyperspectral cameras for monitoring vegetation and soil characteristics.

### *LiDAR*

LiDAR (Light Detection and Ranging) is a technology which has existed conceptually since the 1930s and in application since the 1960s but is now progressing rapidly due to its importance for self-driving vehicle technology (McManamon, 2019). LiDAR units use a narrow beam, or beams of light from an emitter sent in a known direction and measure the time and angle of the beam's return in order to calculate the relative location of what the beam intercepted (McManamon, 2019). If the absolute location of the emitter and receiver are known, then the absolute location of where the beam is also known (McManamon, 2019). This can produce a 3D model of an object through rapid repetition of the process (modern UAV LiDAR units measure more than 100,000 points every second). UAV LiDAR units have three main components:

1. the LiDAR unit itself, which includes the laser emitter and receiver;
2. an inertial monitoring unit (IMU) which detects the angle of the unit, which is an integral part of understanding the relative location of each point; and
3. a GNSS receiver which records the location of the unit, which allows the relative locations of the points to be converted to absolute locations.

The location recorded by the GNSS receiver needs to be compared to the recorded location over a known point by a base-station in a process called post-processing kinematics (PPK), in order to result in accurate location data. LiDAR data needs to be heavily processed after data collection and results in a point-cloud file which will require further processing to get a final digital surface model (DSM) or digital elevation model (DEM).

### *Photogrammetry*

Photogrammetry is a process that can be performed with any camera, where photos taken from a known location and angle can be processed to create an orthomosaic (i.e. a flat, top-down image like those found

on Google Earth), or a 3D reconstruction of an object or area. For UAV photogrammetry, an orthomosaic can be constructed from images taken straight down (nadir), however in order to create a 3D reconstruction of the landscape, the photos must be taken at an angle (off-nadir) (Kyriou, Nikolakopoulos and Koukouvelas, 2021). Photogrammetry processing requires a high level of overlap between each photo (generally 70-90%), so flights tend to take longer than LiDAR for a similar area. Ground control points (GCPs), which are known locations visible from the imagery, are used to georeference the imagery. This is both easier and more difficult than the PPK process for LiDAR, as it requires familiarity with high-accuracy GPS units, but requires one less processing step. The characteristics of the camera, the roughness of the landscape, the flight height, the level of overlap, the accuracy of the GCPs, number of GCPs and the lighting conditions will all effect the quality of the resulting imagery (Mesas-Carrascosa *et al.*, 2016; Rahman *et al.*, 2019; Sangha *et al.*, 2020).

#### *Multispectral and hyperspectral sensors*

Multispectral and hyperspectral sensors are different types of cameras, and photogrammetry methods are required to create an orthomosaic from the images they capture. In order to use the results for vegetation analysis, the background light must be measured and compensated for in analysis, and in order to ensure that the background readings and the sensor images are corresponding, the sensor must be oriented straight down (MicaSense, 2021). This means that multispectral and hyperspectral sensors should not be used for creating 3D models of landforms while also being used for spectral analysis. Both multispectral and hyperspectral sensors capture light which is outside of the visual spectrum, while multispectral sensors capture 5-10 wide bands of spectra (generally RGB, as well as near infrared [NIR] and red edge), hyperspectral sensors capture hundreds of narrow bands of spectra (de Castro *et al.*, 2021).

#### *Applications for reclamation ecology*

LiDAR, photogrammetry, multispectral, and hyperspectral sensors can be used for a wide variety of applications. Both photogrammetry and LiDAR are capable creating high-quality DEMs of unvegetated areas, which makes either approach appropriate for cover placement analysis, erosion monitoring, as well as identification and delineation of opportunistic wetlands. Photogrammetry, either using a regular visual spectrum, multispectral or hyperspectral sensor, can be useful for unvegetated areas to detect differences in the cover material, such as levels of organic matter, or certain forms of mineralization.

Detection of ground surface through vegetation can be difficult for photogrammetry, as the shadows cast by vegetation affect the imagery of underlying areas (Rahman *et al.*, 2019). Any applications which require a clear reading of the ground level through a vegetation should be conducted using LiDAR. For this same reason, LiDAR is better for defining the biomass or LAI of forested ecosystems (Dainelli *et al.*,

2021). This, along with the ability to extract traditional forestry measurements such as gap fraction, stem density, and even height and diameter at breast-height for individual trees using high-density LiDAR, mean that LiDAR is a much more versatile sensor for defining mature forests and other layered vegetation ecosystems (Dainelli *et al.*, 2021). For ecosystems without a defined canopy<sup>1</sup>, the vegetation indices created using multispectral or hyperspectral cameras can be combined DSM and DEM data created using LiDAR or 3d photogrammetry to achieve biomass and LAI (Song, 2013).

Multispectral and hyperspectral data has been used to create indices which correlate with biodiversity of ecosystems, this is particularly effective for ecosystems with flowering species and when imagery is collected multiple times over the course of a growing season (Astor, 2015; Baena *et al.*, 2017; Saarinen *et al.*, 2018; Sankey *et al.*, 2018). These vegetation indices can be used to build proxies for biomass in vegetated systems which do not have complex canopy layering, or to report on health of vegetation. Hyperspectral sensors can be useful for advanced applications such as monitoring of water quality (Becker *et al.*, 2019), which are not possible with a multispectral sensor. The advantage of multispectral sensors is that data collection and processing is much less expensive and complicated than that of hyperspectral sensors.

All remote sensing, whether from UAV or using satellite imagery, must be extensively ground-truthed in order to build and test robust models. With the growing ease of use of some of these tools, rigorous ground-based measurements and research-informed interpretation of data is more important than ever.

### **Case Study – UAV soil amendment mapping at Detour Lake Mine**

Growth of vegetation on waste rock and overburden materials is often slow, often due to the lack of organic matter. Application of an organic amendment can improve nutrient supply and cycling, water availability, and soil biodiversity (Larney & Angers, 2012). Sourcing and application of such an amendment is often complicated and faces numerous operational constraints. The combination of naturally sourced amendments being heterogenous at the source and the thin layer in which amendments are applied over large facilities such as waste rock dumps, can result in a patchy spread of amendment. This can lead to a mosaic of organic matter concentrations and quality. Understanding the heterogeneity of reclamation-cover placement is essential for the interpretation of revegetation studies on such systems. Mapping the spatial distribution of reclamation covers, such as a peat-mineral mix (PMM), using on-the-ground methods can be time-consuming and expensive. UAVs offer an innovative, time-saving and cost-effective approach to delineating placement of these covers.

---

<sup>1</sup> Such as sparsely forested or shrubby.

Integral Ecology Group conducted a UAV survey of PMM distribution on a large (5.3-hectares) constructed plateau at Detour Lake Mine (located in northeastern Ontario) in 2020. The facility is a waste-rock stockpile, capped with overburden materials, which is designed as a cover and revegetation trial to establish reclamation methods which can be applied to future mine-planning. The trial is designed to measure a wide variety of metrics, including mortality and growth of planted seedlings, ingress of native species, cover hydrology, and carbon and water fluxes in and out of the system. The plateau of the facility, which makes up the study area, was covered with a 0.3 m overburden growth medium which consisted of a peat mineral mix (PMM) targeted to have approximately 20-30% peat by volume (BGC 2020). The peat and mineral components of the mix were salvaged together and mixed through the dumping and spreading process, and additional peat was dumped and spread in order to achieve the desired proportions (BGC 2020). Due to the uneven distribution of peat and mineral soil in amendment stockpiles, the process resulted in a spatially heterogeneous distribution of peat. Though for operational reclamation, this degree of patchiness would have been appropriate, it represented a major covariate which could disrupt learnings from the trial area if not accounted for. The use of a UAV to create a spatially-explicit map of organic matter distribution will allow its inclusion as a variable in relevant analysis. Vegetation, hydrological and flux measurements are still being gathered at the time of writing, so only seedling mortality is currently available for comparison with peat content.

#### *UAV Parameters and Mission Planning*

Aerial images of the study area were collected using a DJI Mavic Pro equipped with a 12 Megapixel RGB camera with a 79-degree field of view. The Mavic Pro is a quadcopter drone, small enough to fit in a backpack, with batteries small enough to be permitted on commercial flights. It weighs approximately 740 grams and can be flown safely and easily in non-restricted airspace over an unpopulated area with a Basic UAV Pilot's license.

The UAV mission was planned using the Pix4D Capture app, using the following settings:

- 70% side overlap and 80% front overlap
- 65-meter altitude
- 75-degree camera angle (90 degrees would be straight down)
- Double grid formation to create both an orthomosaic and a 3D model of the area

The total area mapped was 19-hectares and had a flight time of 58 minutes, requiring four battery changes. 1250 aerial photos were collected as a result. The total area mapped was significantly larger than

the study area (5.3-hectares) – flight time would have been significantly reduced if only the study area was mapped<sup>2</sup>.

### *UAV Data Analysis*

The workflow for analysis can be generalized into four main steps: (1) aerial image processing; (2) orthomosaic analysis; (3) accuracy assessment; and (4) application.

1. Aerial image processing. Aerial images were processed into an orthomosaic using Agisoft Metashape Professional Edition 1.7.3. Agisoft uses structure-from-motion (SFM) to align photos, reconstruct 3D point clouds, and produce Digital Elevation Models (DEM) and orthomosaics.
2. Orthomosaic analysis. Orthomosaic analysis was performed using OBIA, a workflow found within the Orfeo Toolbox<sup>3</sup>. OBIA analyses images at the object level rather than the pixel level and uses spectral, textural, and contextual information to group pixels in an image. OBIA works well for very high resolution RGB UAV imagery and can help reduce the effects of shadow (De luca et al., 2019). OBIA has three main steps:
  - a. Segmentation. The orthomosaic is segmented into a vector dataset based on groupings of similar pixels where every polygon represents an object.
  - b. Training and control samples. Training and control samples are manually created in a GIS environment. The training samples will inform the classification what the characteristics of high-peat and low-peat polygons are, while the control samples will check the accuracy of the classification (step 2c). Training and control samples were categorised into the following land cover classes: (1) high-peat; (2) medium-high-peat; (3) medium-low-peat; (4) low-peat; (5) waste-rock.
  - c. Classification. A supervised classification function is run using the Random Forest (RF) algorithm through the Orfeo Toolbox. The final output is a polygon layer where the polygons are classified as one of the five land cover classes. For the purposes of this case study, high-peat and medium-high-peat land cover classes were grouped together to represent high-peat polygons, while medium-low-peat, low-peat, and waste-rock land cover classes were grouped together to represent low-peat polygons.

---

<sup>2</sup> The additional mapped area was included in the data collection to include trial areas which are unrelated to this case-study.

<sup>3</sup> The Orfeo Toolbox is an open-source multi-purpose remote sensing toolbox which can be used for basic pre-processing or running advanced remote sensing algorithms (Grizonnet et al., 2017).

3. Accuracy assessment. A confusion matrix<sup>4</sup> and kappa value<sup>5</sup> are generated from the RF classification - these are the most common measures of accuracy for remotely sensed data (Morales-Barquero et al., 2019). User's, producer's, and overall accuracy are then calculated using the confusion matrix.
4. Application. The proportion of high-peat and low-peat polygons within the PSPs were used to classify each PSP as high or low-peat. If a PSP had a peat content of 50% or greater it was classified as high-peat and if it had less than 50% peat content it was classified as low-peat. Seedling survival rates were measured at each PSP, and comparisons between high-peat and low-peat PSPs were analyzed by analysis of variance.

#### *Orthomosaic interpretation*

Visual inspection of the 3D model and orthomosaic (~1.5 cm/px) produced in Agisoft can provide useful information before any additional analysis is performed. Figure 1 highlights the heterogenous distribution of PMM, with the browner areas containing high-peat and the greyer areas containing low-peat.

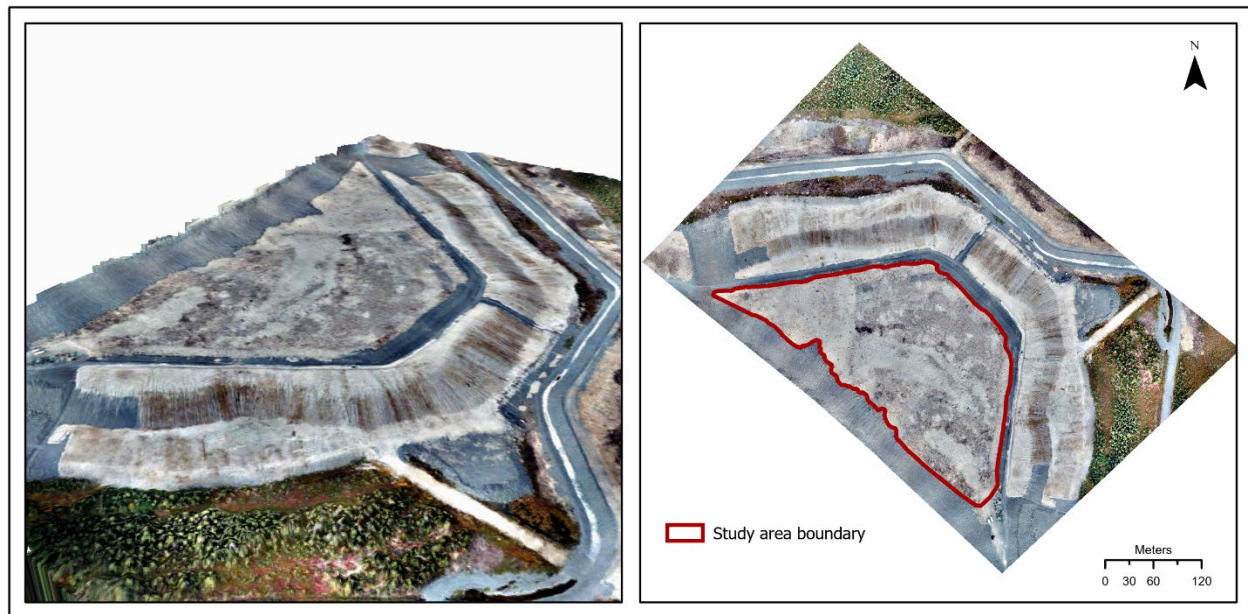


**Figure 1. 3D model (left) and orthomosaic (right) of the study area.**

<sup>4</sup> A confusion matrix displays correct (and sometimes also incorrect) modeled outcomes for each given known (measured) outcome.

<sup>5</sup> Kappa value is a measure of how close the modelled classification outcome is to the correct outcome.

### *Orthomosaic analysis*

Figure 2 is the result of segmenting the orthomosaic (step 2a); each segment or polygon is now an individual object. The training points (step 2b) assign objects a land cover class based on the polygons they overlap. Check points (step 2b) will then assess the accuracy of the training algorithm by comparing the analyst classification with the RF algorithm classification.

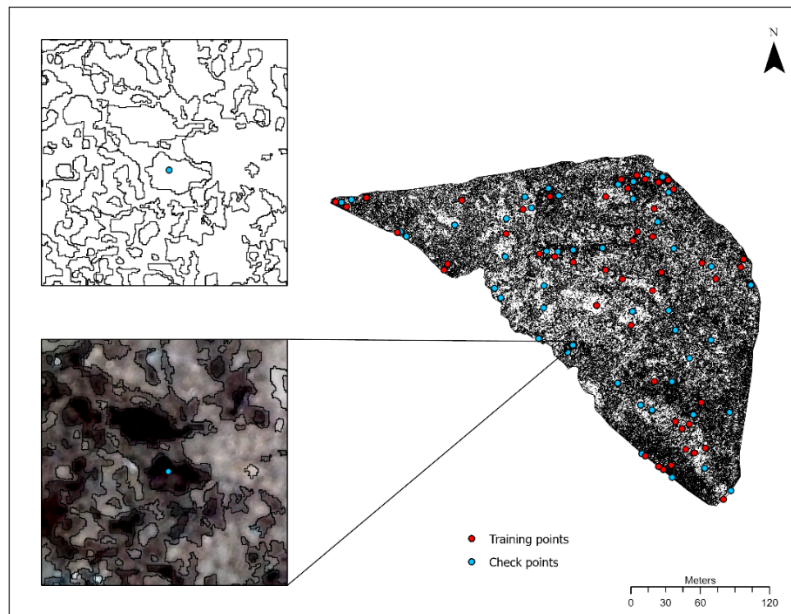


**Figure 2. Distribution of training and check points over the segmented study area.**

Figure 3 is the final output of the orthomosaic analysis (step 2c). All of the polygons or ‘objects’ from the segmentation stage have been classified as having high or low-peat. The patchy distribution of PMM is now apparent.



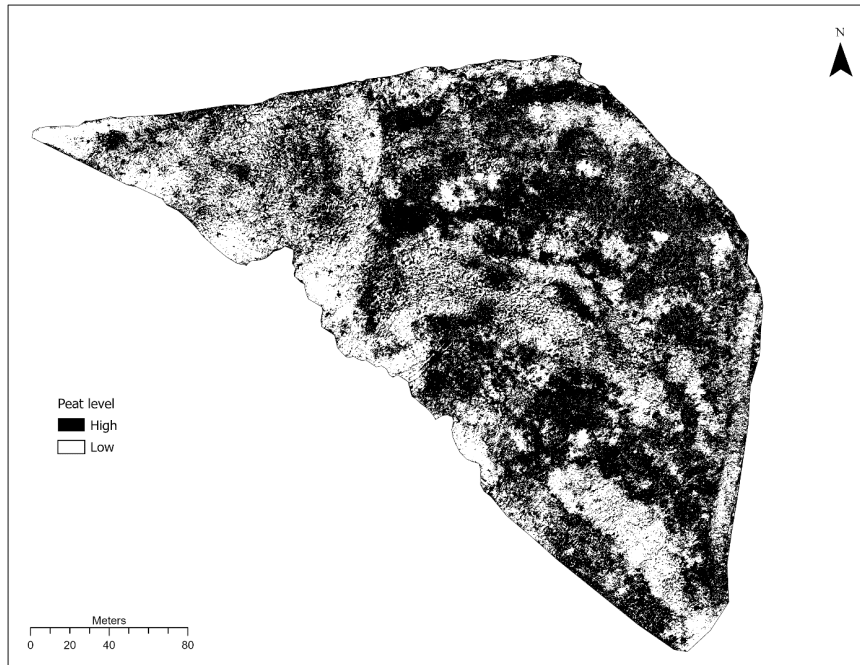


**Figure 3. Areas of high (black) and low (white) peat content on the study area.**

#### *Accuracy assessment*

Table 1. reports the confusion matrix for the accuracy assessment. The overall accuracy for the RF classification is 84.51% while the kappa value is 0.81.

**Table 1. Confusion matrix for the Random Forest classification algorithm.**

	Reference Data					Total	User's Accuracy
	1	2	3	4	5		
<b>Classified</b>	1	8	0	0	0	8	100
	2	0	4	3	0	7	57.14
	3	0	1	6	0	8	75.00
	4	0	0	0	8	8	100.00
	5	0	1	0	0	7	87.50
<b>Total</b>	8	6	9	8	8	39	
<b>Producer's accuracy</b>	100	66.67	66.67	100.00	87.50		

*Correlation with seedling survival*

Results indicated a significantly ( $\alpha = 0.05$ ) higher survival for conifer seedlings planted in high-peat areas than those planted in low-peat areas, with survival approximately 15% higher for pine and 22% higher for spruce in high-peat areas Figure 4.

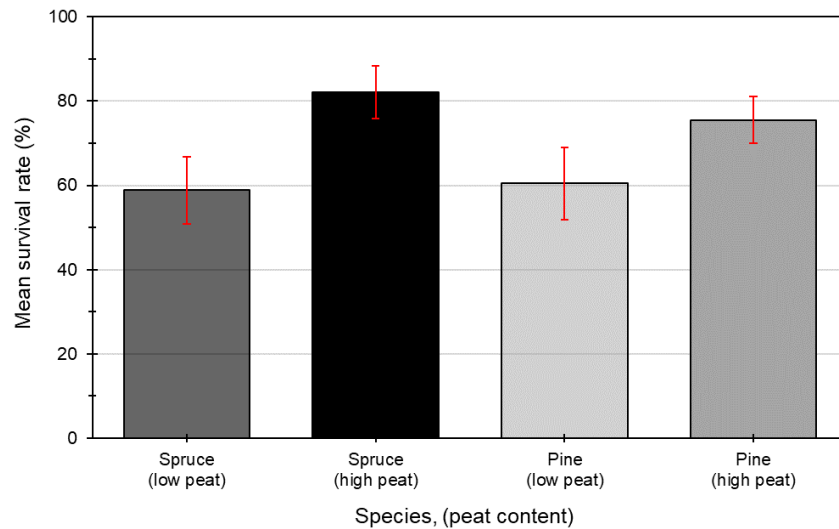


**Figure 4. Seedling average survival rate by species and peat content within the study area (error bars indicate the standard error of the estimate of the mean).**

## Discussion

This case study demonstrates a practical method of using a UAV to obtain information from which to inform revegetation efforts. OBIA of the UAV derived orthomosaic and the resulting quantification of PMM in the study area allowed the distribution of the reclamation-cover to be included in an overall analysis of seedling survival rates as an important variable. Although there are likely other important covariates impacting seedling survival, the results of this case study suggest the application of PMM in future reclamation attempts at the Detour Lake Mine would likely lead to an increased rate of seedling survival over the initial year after planting.

This case study is also an example of the value a relatively affordable UAV can bring to reclamation efforts. The Mavic Pro cost approximately \$1500, making it one of the more affordable UAV options available, yet provided valuable information which otherwise would have been excluded from the seedling survival rate analysis. Although Agisoft, the photogrammetry software, requires a paid subscription, all other processing was performed using open-source software. Orfeo Toolbox is just one example of an open-source software that can be used for this kind of analysis but there are plenty of others available, including QGIS, a popular GIS platform that has supervised classification plug-ins available.

The limitations of this study are similar to all UAV and remote sensing limitations – achieving high classification accuracy. Limitations were addressed by running multiple classifications with different settings to decrease reported errors, and visually inspecting each classification to ensure it agreed with

what the visual eye could perceive. While the accuracy of the classification could be improved, the results were more than satisfactory for the purposes of this study. The Mavic Pro and its camera, however, were pushed to the limits, and ultimately, there is a relative increase in equipment cost and technical ability in achieving higher accuracies.

## References

- Astor, T. (2015) *Hyperspectral and multispectral remote sensing for mapping grassland vegetation*. doi: 10.13140/RG.2.1.2745.4564.
- Baena, S. *et al.* (2017) “Identifying species from the air: UAVs and the very high resolution challenge for plant conservation,” *PLOS ONE*, 12(11). doi: 10.1371/journal.pone.0188714.
- Becker, R. H. *et al.* (2019) “Unmanned aerial system based spectroradiometer for monitoring harmful algal blooms: A new paradigm in water quality monitoring,” *Journal of Great Lakes Research*, 45(3), pp. 444–453. doi: <https://doi.org/10.1016/j.jglr.2019.03.006>.
- de Castro, A. I. *et al.* (2021) “UAVs for Vegetation Monitoring: Overview and Recent Scientific Contributions,” *Remote Sensing*, 13(11). doi: 10.3390/rs13112139.
- Dainelli, R. *et al.* (2021) “Recent Advances in Unmanned Aerial Vehicles Forest Remote Sensing—A Systematic Review. Part II: Research Applications,” *Forests*, 12(4). doi: 10.3390/f12040397.
- De Luca, G., N. Silva, J. M., Cerasoli, S., Araújo, J., Campos, J., Di Fazio, S., & Modica, G. (2019). Object-based land cover classification of cork oak woodlands using UAV imagery and orfeo ToolBox. *Remote Sensing (Basel, Switzerland)*, 11(10), 1238.
- Grizonnet, M., Michel, J., Poughon, V., Inglada, J., Savinaud, M., & Cresson, R. (2017). Orfeo ToolBox: Open source processing of remote sensing images. *Open Geospatial Data, Software and Standards*, 2(15)
- Kyriou, A., Nikolakopoulos, K. and Koukouvelas, I. (2021) “How Image Acquisition Geometry of UAV Campaigns Affects the Derived Products and Their Accuracy in Areas with Complex Geomorphology,” *ISPRS International Journal of Geo-Information*, 10(6). doi: 10.3390/ijgi10060408.
- Larney, F. J., & Angers, D. A. (2012). The role of organic amendments in soil reclamation: A review. *Canadian Journal of Soil Science*, 92(1), 19-38.
- McManamon, P. F. (2019) “History of LiDAR,” in *LiDAR Technologies and Systems*. SPIE. doi: 10.1117/3.2518254.ch2.
- Mesas-Carrascosa, F.-J. *et al.* (2016) “An Analysis of the Influence of Flight Parameters in the Generation of Unmanned Aerial Vehicle (UAV) Orthomosaics to Survey Archaeological Areas,” *Sensors*, 16(11). doi: 10.3390/s16111838.
- MicaSense (2021) *Best practices: Collecting Data with MicaSense Sensors*, <https://support.micasense.com/hc/en-us/articles/224893167-Best-practices-Collecting-Data-with-MicaSense-RedEdge-and-Parrot-Sequoia>.

- Morales-Barquero, L., Lyons, M., Phinn, S., & Roelfsema, C. (2019). Trends in remote sensing accuracy assessment approaches in the context of natural resources. *Remote Sensing (Basel, Switzerland)*, 11(19), 2305.
- Park, S. and Choi, Y. (2020) “Applications of Unmanned Aerial Vehicles in Mining from Exploration to Reclamation: A Review,” *Minerals*, 10, p. 663. doi: 10.3390/min10080663.
- Rahman, M. M. *et al.* (2019) “A workflow to minimize shadows in UAV-based orthomosaics,” *Journal of Unmanned Vehicle Systems*, 7(2), pp. 107–117. doi: 10.1139/juvs-2018-0012.
- Saarinen, N. *et al.* (2018) “Assessing Biodiversity in Boreal Forests with UAV-Based Photogrammetric Point Clouds and Hyperspectral Imaging,” *Remote Sensing*, 10(2). doi: 10.3390/rs10020338.
- Sangha, H. S. *et al.* (2020) “Impact of camera focal length and sUAS flying altitude on spatial crop canopy temperature evaluation,” *Computers and Electronics in Agriculture*, 172, p. 105344. doi: <https://doi.org/10.1016/j.compag.2020.105344>.
- Sankey, T. T. *et al.* (2018) “UAV hyperspectral and lidar data and their fusion for arid and semi-arid land vegetation monitoring,” *Remote Sensing in Ecology and Conservation*, 4(1). doi: 10.1002/rse2.44.
- Song, C. (2013) “Optical remote sensing of forest leaf area index and biomass,” *Progress in Physical Geography: Earth and Environment*, 37(1). doi: 10.1177/0309133312471367.
- Valavanis Kimon P. and Vachtsevanos, G. J. (2015) “UAV Mission and Path Planning: Introduction,” (ed.) *Handbook of Unmanned Aerial Vehicles*. Dordrecht: Springer Netherlands, pp. 1443–1446. doi: 10.1007/978-90-481-9707-1\_143.